Environ. Sci. Technol. **1998**, *32,* 3893−3900

Neptunium and Plutonium Solubilities in a Yucca Mountain Groundwater

D. WES EFURD, WOLFGANG RUNDE,* JOE C. BANAR, DAVID R. JANECKY, JOHN P. KASZUBA, PHILLIP D. PALMER, FRED R. ROENSCH, AND C. DREW TAIT

Los Alamos National Laboratory, Chemical Science and Technology Division, Los Alamos, New Mexico 87545

Solubilities of neptunium and plutonium were studied in J-13 groundwater (ionic strength of about 3.7 mmol; total dissolved carbonate of 2.8 mmol) from the proposed Yucca Mountain Nuclear Waste Repository site, Nevada, at three different temperatures (25, 60, and 90 °C) and pH values (6.0, 7.0, and 8.5). Experiments were performed from both over- and undersaturation at defined CO_2 partial pressures. The solubility of ^{237}Np from oversaturation ranged from a high of $(9.40 \pm 1.22) \times 10^{-4}$ M at pH 6.0 and 60 °C to a low of $(5.50 \pm 1.97) \times 10^{-6}$ M at pH 8.5 and 90 °C. The analytical results of solubility experiments from undersaturation (temperatures of 25 and 90 °C and pH values 6, 7, and 8.5) converged on these values. The $^{239/240}Pu$ solubilities ranged from $(4.70 \pm 1.13) \times 10^{-8}$ M at pH 6.0 and 25 °C to $(3.62 \pm 1.14) \times 10^{-9}$ M at pH 8.5 and 90 °C. In general, both neptunium and plutonium solubilities decreased with increasing pH and temperature. Greenish-brown crystalline $Np_2O_5 \cdot xH_2O$ was identified as the solubility-limiting solid using X-ray diffraction. A mean thermodynamic solubility product for $Np_2O_5 \cdot xH_2O$ of log $K°_{sp} = 5.2 \pm 0.8$ for the reaction $Np_2O_5 \cdot xH_2O + 2\ H^+ \rightleftharpoons 2NpO_2^+ + (x+1)H_2O$ at 25 °C was calculated. Sparingly soluble Pu(IV) solids, $PuO_2 \cdot xH_2O$ and/or amorphous plutonium(IV) hydroxide/colloids, control the solubility of plutonium in J-13 water.

Introduction

The site at Yucca Mountain (YM), NV, is being characterized to determine its suitability as a potential repository for high-level nuclear waste in the United States. As part of this characterization, risk assessment considers worst-case scenarios such as the consequences of water intrusion into the repository. The rate of groundwater flow through the waste is expected to be sufficiently slow to permit saturation of water with radionuclides; therefore, solubility and speciation data define the source term for transport and retardation processes (*1*). The technical position of the U.S. Nuclear Regulatory Commission (NRC) (*2*) requires that if radionuclide solubility is used as a factor in limiting radionuclide release, solubility experiments must be designed to use site-specific conditions. Water from well J-13 is a reference water for the unsaturated zone (UZ) near the proposed emplacement area (Table 1). Typical of many groundwaters in the western United States, J-13 water is fairly low in ionic strength (mmol range), with carbonate and hydroxide as predominant potential ligands (*3*).

TABLE 1. Well J-13 Water Composition (*3*)

species	concentration (mM)	species	concentration (mM)
Na^+	1.96	F^-	0.11
K^+	0.136	Cl^-	0.18
Li^+	0.009	NO_3^-	0.16
Ca^{2+}	0.29	SO_4^{2-}	0.19
Mg^{2+}	0.072	SiO_2	1.07
Mn^{2+}	0.00002	alkalinity	2.3 mequiv/L
$Fe^{2+/3+}$	0.0008	total carbonate	2.81
Al^{3+}	0.0010		
pH	7.0	E_h	700 mV[a]

[a] We remeasured the redox potential of J-13 water at pH 7 and the Ar/CO_2 gas mixture used in the solubility experiments with a combined platinum redox and Ag/AgCl reference electrode (Orion, model 96-78-00). We obtained a much lower redox potential, namely, 430 ± 50 mV. We used this value for our solubility calculations.

For meaningful interpretation of solubility data, detailed knowledge of the nature of the solubility controlling solid phase along with concentration and composition of solution species at steady state is required. Steady state is assumed to be established when pH and actinide concentration remain stable for several weeks (*2*). However, precipitated solids may become less soluble as they recrystallize from initially formed disordered structures toward ordered structures, thereby lowering the free energy of the solid. Such a change may be kinetically controlled and not appear in the experiment or in nature even after several years. Consequently, the solids formed in the experiments may not represent the thermodynamically most stable solids with the lowest solubility. Thus, solubility studies provide an upper concentration limit of actinides in a potential release scenario from a proposed nuclear waste repository. Radiolysis may also affect the crystallization and solubility of actinide solids.

Neptunium and plutonium are two of the radionuclides of concern in long-term emplacement of nuclear waste (*1*, *4*, *5*). Nitsche et al. (*6*, *7*) studied their solubilities in YM waters, J-13 ($I \approx 3.7$ mmol; $[CO_2]_t = 2.8$ mmol) and UE-25p#1 ($I \approx 20$ mmol; $[CO_2]_t = 15.3$ mmol), as a function of pH and temperature. However, the experiments were continually titrated to maintain the pH and produced solutions with ionic strengths too high to accurately describe the low ionic strength YM waters. As a result of the significantly increased sodium concentrations in the experiments, a mixture of metastable sodium neptunyl(V) carbonates and Np_2O_5 were formed simultaneously, impeding the proper determination of upper neptunium solubility limits and the meaningful thermodynamic interpretation of the obtained data. In addition, there are inconsistencies of about 1 order of magnitude in the series of reported plutonium solubility values. These early experiments did, however, point to the prime importance of neptunium and plutonium in YM total system performance assessment (TSPA) (*8*, *9*), because of both the relatively high solubility and low sorption behavior of neptunium and the potential simultaneous existence of multiple oxidation states and therefore complicated solubility behavior of plutonium.

This study provides experimentally determined solubility limits for neptunium and plutonium that may be used to calculate their transport along potential transport pathways from the repository to the accessible environment, as required in the Yucca Mountain Site Characterization Plan (*10*). Over-

* To whom correspondence should be addressed. E-mail: runde@lanl.gov; phone: (505)667-3350; fax: (505)665-4955.

10.1021/es980591h CCC: $15.00
Published on Web 11/06/1998

TABLE 2. Concentrations (in %) of Carbon Dioxide Gas in Argon Used To Maintain a Total Dissolved Carbonate Concentration of 2.8×10^{-3} M in J-13 Groundwater at Different pH and Temperatures

	25 °C	60 °C	90 °C
pH 6.0	6.06 ± 0.02	9.67 ± 0.02	18.58 ± 0.02
pH 7.0	1.57 ± 0.02	2.35 ± 0.02	4.05 ± 0.02
pH 8.5	0.060 ± 0.0001	0.090 ± 0.001	0.140 ± 0.001

and undersaturation experiments were performed, and solution concentrations were measured as a function of time to demonstrate steady-state conditions and an approach to equilibrium. The pH values and temperatures in the solubility experiments were selected to bracket the range of conditions that represent lower and upper limits expected at the site in J-13 water. The experimental results are interpreted with thermodynamic modeling and integrated into our current understanding of neptunium and plutonium geochemistry.

Experimental Section

J-13 groundwater was filtered through 0.05 μm polycarbonate membrane filters (Nuclepore Corp., Pleasanton, CA). The water's natural carbon dioxide (CO_2) partial pressure could not be preserved during storage and filtration. Thus, the natural state of the well water's total dissolved carbonate, 2.8×10^{-3} M (*3*), was induced by reequilibrating the water at each individual pH with defined argon/CO_2 gas mixtures. The necessary amount of CO_2 at a given pH and temperature (Table 2) was calculated from Henry's law constant, the dissociation constants of carbonic acid (*11*), and the Davies equation. If the constant at the given temperature was not available, it was derived by interpolation of adjacent values.

The solubility experiments were performed in 135-mL cells constructed of polyether ketone (PEEK). Each cell had a sealed port at the top that could be removed to withdraw samples and measure pH and was equipped with 1/8 in. diameter Teflon line for addition of the appropriate argon/CO_2 mixture. The system was designed to minimize significant evaporative loss of the solution, especially at elevated temperature. Measured evaporative losses ranged from 5 to 10 mL (<10%) for the duration of the experiments. Up to nine cells were accommodated in a temperature regulation system consisting of an aluminum block that was insulated with extruded polystyrene (U C Industries, Parsippsany, NJ) and natural cork. The aluminum block was mounted on an orbital shaker (Lab-Line Inc., Melrose Park, IL), and all solutions were shaken continuously at approximately 100 rpm. Silicone fluid (Dow Corning Corporation, Midland, MI, 550 High-Temperature Silicone Fluid) heated by a heating circulator (VWR Scientific, model 1137) was pumped through channels in the aluminum block allowing control of temperatures to within less than 1 °C. The whole experimental setup was installed in argon atmosphere gloveboxes (Plas Labs, Lansing, MI, model 818-GBB).

The actinide stock solutions were prepared by dissolving ultrapure neptunium and plutonium metal in perchloric acid. The neptunium stock solution was prepared by placing 1.36 g of electrorefined neptunium metal in a 125-mL narrow-mouth Teflon FEP bottle and adding 20 mL of ultrapure perchloric acid (Seastar Chemicals Inc.). The plutonium stock solution was prepared by placing 0.50688 g of National Bureau of Standards Standard Reference Material 949f in a 125-mL narrow-mouth Teflon FEP bottle and adding approximately 10 mL of ultrapure perchloric acid (Seastar Chemicals Inc.). Each sample was heated until the neptunium or plutonium metal completely dissolved, and the volume was reduced to approximately 0.5 mL. The samples were then cooled to room temperature, purged with argon until the excess perchloric acid was evaporated, diluted with deionized water, and adjusted to 1 M with respect to perchloric acid. The solutions were digested in an approximately 60 °C water bath overnight and filtered through a 0.2-mm nylon syringe filter unit (Gelman Sciences) into a 30-mL narrow-mouth Teflon FEP bottle. Filtration removed suspended particulate material, e.g., dust or silica, that could adsorb the actinide ions. To adjust the pH to the desired value, we added aliquots of sodium hydroxide solution (0.05 M) before and 0.05 M perchloric acid and/or 0.05 M sodium hydroxide after addition of the acidic actinide stock solution to the J-13 water. These additions of acid and base increased the total Na^+ content between 2.3 and 4.1 times that of J-13 water, but the ionic strength of the J-13 water remained below 0.01 M. This contrasts markedly with the solubility studies for YM waters reported earlier, where the pH was kept constant with the continual addition of acid and base using a pH-stat, resulting in a final ionic strength being 1−2 orders of magnitude higher than J-13 (*6*, *7*).

In addition to the solubility experiments from oversaturation, the neptunium solubility in J-13 water was determined from undersaturation. Solid phases formed in oversaturation experiments were recontacted with fresh J-13 water equilibrated with the appropriate CO_2/argon gas mixture, and the pH was adjusted to 6, 7, and 8.5 at 25 °C and 90 °C. These experiments allowed the original composition of J-13 water to be maintained even more closely than in the oversaturation experiment since no addition of NaOH solution was necessary to neutralize the acidic neptunium or plutonium stock solution.

The solubility experiments were allowed to equilibrate for several months without further addition of acid or base. Achievement of steady-state conditions was monitored by sampling aliquots of the solution phases and analyzing for the respective actinide concentration as a function of time. Centricon-30 filters (regenerated cellulose polymer for low retention/sorption, Millipore Corp., Bedford, MA), with a calculated pore size of 4.1 nm, were used for separating solid and solution phases. The centrifuge (high-speed centrifuge, Speedfuge SFG10K, Savant Instruments Inc.) was preheated to the appropriate temperature, and the centrifuge's walls were insulated with approximately 1 cm of extruded polystyrene (UC Industries, Parsippsany, NJ). To ascertain the complete phase separation and minimal adsorption on the filters during the preparation of the solution assays, a series of filtration tests was conducted. One filter was used per solution to filter consecutive 500-μL aliquots until a constant concentration in the filtrate was obtained. Assays indicated that 2000-μL preconditioning volumes were ultraconservative, and the active sites on the filters were saturated with the first 1000 μL of solution for all temperatures and pH values for both neptunium and plutonium. Each filtrate was then acidified to minimize subsequent concentration reduction due to sorption.

Concentration measurements of the filtrates were made by counting aliquots that were stippled onto stainless steel disks, evaporated to dryness under a heat lamp, flamed to dull red, and counted on an α-scintillation counter (Eberline Instrument Corporation, Santa Fe, NM, model SAC-4). The counting efficiency of the scintillation counter was determined by counting plutonium samples traceable to NIST. The pH and carbonate concentration of each cell were established only initially, and no pH adjustments were made during the duration of the experiments. The pH of the solution was measured with each sampling with a Ross combination pH electrode (Orion Research Inc., Orion model 611) and a pH/millivolt meter (Orion Research Inc.). The pH electrode was calibrated before the pH measurements

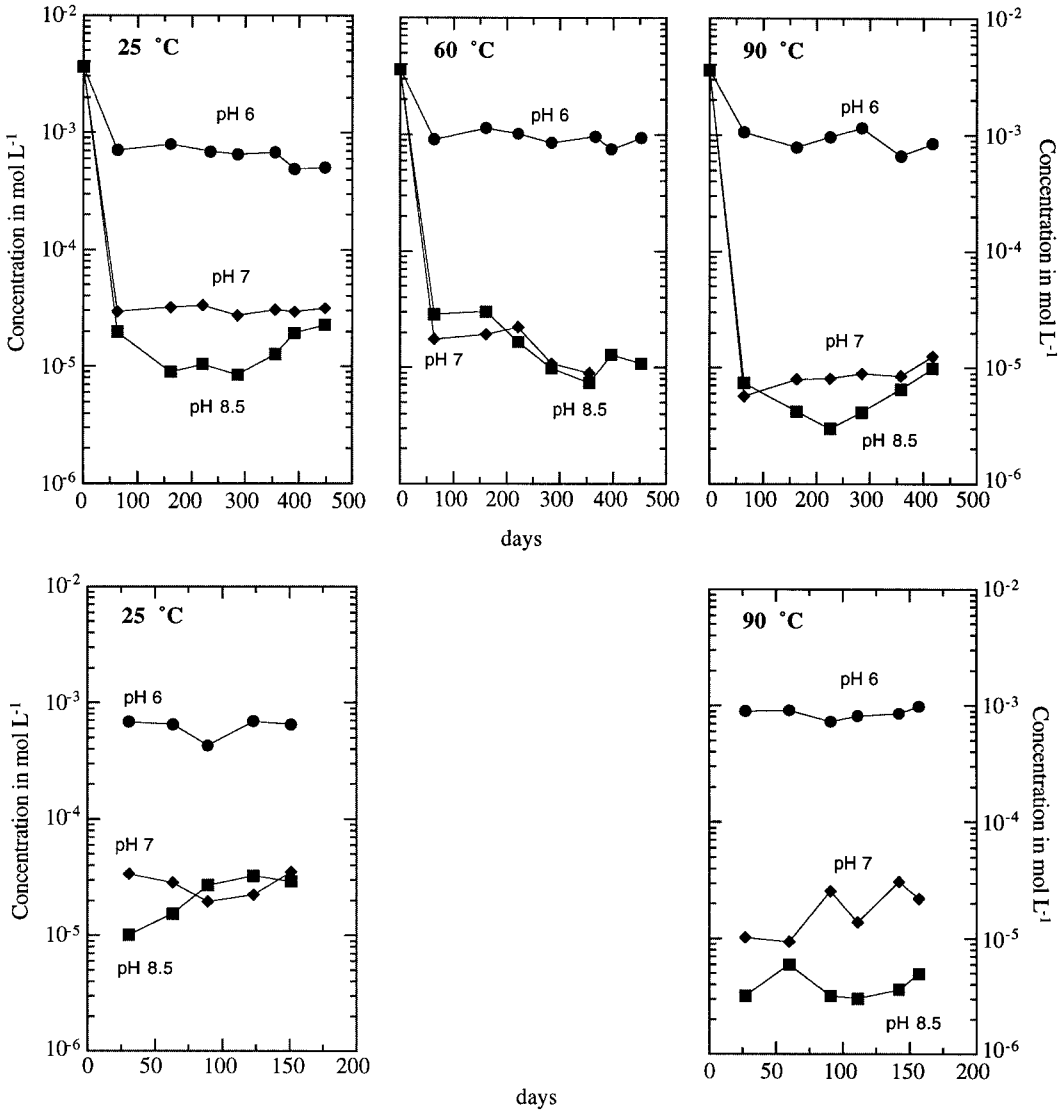

FIGURE 1. Np solubility in J-13 water from oversaturation (top) and undersaturation (bottom) at (●) pH 6, (◆) 7, and (■) 8.5 and 25, 60, and 90 °C.

using commercially available VWR standard solutions (pH = 4.00, 7.00, and 10.02).

At the end of the solubility experiments, the neptunium and plutonium precipitates were dried under the corresponding CO_2 atmosphere and were analyzed using X-ray powder diffraction (XRD) and diffuse reflectance spectroscopy. For the XRD measurements, a few milligrams of each actinide precipitate was placed on a Teflon holder, covered with Kapton foil, and secured with an O-ring to prevent contamination. The spinning sample was irradiated with Cu-$K_{\alpha 1}$ radiation generated by the INEL CPS-120 (INEL Inc.) X-ray powder diffractometer. To calibrate the instrument, the powder pattern of Si (NBS Standard Reference Material No. 640, CAS Registry No. 7440-21-3) was collected before and after the sample analysis and compared with data from the JCPDS card no. 27-1402. The samples to be investigated by diffuse reflectance spectroscopy were placed in a quartz cell and sealed by a Teflon plug. Reflectance measurements were carried out on a Lambda 19 (Perkin-Elmer) spectrophotometer with a slit width of 1 nm, scan speed of 60 nm/min, and 0.5 nm data acquisition increments. Geochemical modeling and thermodynamic calculations were performed with the EQ3nr code (4025v7.233) (*12, 13*) using the b-dot extended Debye−Huckel model (*14*) and a standard thermodynamic database (LLNL Combination Database DATA0.COM.V8.R6, released December 1996). The latter is based on neptunium data from Lemire (*15*) and on plutonium data from Lemire and Tremaine (*16*) excluding the pentahydroxo species of Np(IV) and Pu(IV).

Results and Discussion

Neptunium Solubility. As expected, the average neptunium solubility generally decreased with increasing pH (Figure 1), following the known trend of neptunium solubilities up to approximately pH 8 in carbonate-containing media (*17*−*21*) and up to approximately pH 12 in carbonate-free systems (*20, 22*−*24*). Results of the neptunium solubility experiments from both over- and undersaturation converge to the same steady-state concentrations (Figure 1, Table 3). At the conditions of these experiments, speciation model calculations indicate NpO_2^+, $NpO_2(OH)$, and $NpO_2CO_3^-$ as the predominant species in solution. Further increase in pH would result in increasing neptunium solubility due to the formation of higher complexed anionic neptunium species in solution. With increasing temperature, a slight decrease in solubility is observed at pH 7 and pH 8.5, while at pH 6 the neptunium solubility remains approximately constant. The soluble neptunium concentrations are similar at pH 7 and pH 8.5, while at pH 6 the solubility is about 1−2 orders higher depending on the temperature. At pH 8.5, the

TABLE 3. Averaged Concentrations of ^{237}Np (in mol L^{-1}) as a Function of pH and Temperature As Measured from Oversaturation (after 450 days Equilibration) and Undersaturation (after 151 days Equilibration) in This Study in Comparison with Literature Data (*6*, *7*)[a]

	pH 6	pH 7	pH 8.5
25 °C			
oversaturation	$(6.5 \pm 1.1) \times 10^{-4}$	$(3.1 \pm 0.2) \times 10^{-5}$	$(1.5 \pm 0.6) \times 10^{-5}$
undersaturation	$(6.5 \pm 1.0) \times 10^{-4}$	$(2.9 \pm 0.7) \times 10^{-5}$	$(1.5 \pm 0.3) \times 10^{-5}$
[lit.]	$(5.3 \pm 0.1) \times 10^{-3}$	$(13 \pm 3) \times 10^{-3}$	$(4.4 \pm 0.7) \times 10^{-3}$
60 °C			
oversaturation	$(9.4 \pm 1.2) \times 10^{-4}$	$(1.6 \pm 0.6) \times 10^{-5}$	$(1.7 \pm 0.9) \times 10^{-5}$
undersaturation			
[lit.]	$(6.4 \pm 0.4) \times 10^{-3}$	$(9.8 \pm 1.0) \times 10^{-4}$	$(1.0 \pm 0.1) \times 10^{-5}$
90 °C			
oversaturation	$(9.1 \pm 1.8) \times 10^{-4}$	$(8.6 \pm 2.3) \times 10^{-6}$	$(5.8 \pm 2.5) \times 10^{-6}$
undersaturation	$(8.7 \pm 0.9) \times 10^{-4}$	$(9.3 \pm 1.9) \times 10^{-6}$	$(5.9 \pm 2.1) \times 10^{-6}$
[lit.]	$(1.2 \pm 0.1) \times 10^{-3}$	$(1.5 \pm 0.4) \times 10^{-4}$	$(8.9 \pm 0.4) \times 10^{-5}$

[a] Uncertainties are given as one standard deviation.

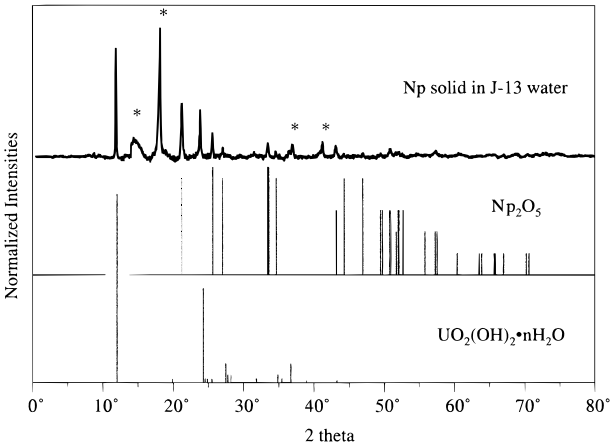

FIGURE 2. X-ray diffraction pattern of the neptunium solid found in J-13 water at 90 °C in comparison with literature data of Np_2O_5 (*26*) and hydrated U(VI) hydroxide (*29*). Bragg reflections caused by the sample arrangement are marked with an asterisk. The observed peaks in the experimental sample suggest a hydrated neptunium(V) oxide.

neptunium concentrations were observed to decrease in the first 250 days, followed by an increase in concentration for the 25 and 90 °C oversaturation experiments (all other oversaturation experiments either showed the expected decreasing or constant concentration trend throughout the 450 days of the equilibration). Because the solid phase was not investigated during these events, this trend at pH 8.5 cannot be explained conclusively at the present time.

The neptunium precipitates formed were dark greenish brown. X-ray diffraction data showed only a few broad Bragg reflections for neptunium solids formed at low temperature, while increased temperature induced sharper peaks at 90 °C (Figure 2). The powder patterns obtained are generally consistent with the reported data for both Np_2O_5 and Np_3O_8 (*25*, *26*) with some additional peaks that do not correspond to these solids. The formation of the mixed oxide Np_3O_8 is not likely, and in fact, the existence of a Np_3O_8 phase has been discounted in studies (*27*, *28*) after those of Cohen et al. (*25*, *26*). The observed diffraction patterns do not match other reported neptunium solids, and the existence of a sodium neptunyl carbonate could be excluded. The additional peaks do match well with the Bragg reflections of hydrated uranium(VI) hydroxide (*29*). It should also be noted that the reported X-ray powder pattern of Np_2O_5 was obtained from solids produced by the reaction of Np(V) in molten lithium perchlorate at 260 °C in the absence of water. In contrast, hydrated neptunium(V) oxide would be expected to form in aqueous solution experiments. Thus, through comparison with the literature for neptunium solids and hydrated uranium(VI) hydroxide, we assign the principle lines in the XRD of the neptunium precipitates to $Np_2O_5 \cdot xH_2O$. While we assign the additional peaks caused by intercalated water molecules and the further separation of the neptunium oxide layers, we cannot exclude the presence of amorphous neptunium(V) hydroxide by X-ray diffraction (*30*).

We used the solubility data in J-13 water to calculate the solubility product of the solid phase $Np_2O_5 \cdot xH_2O$. At pH 8.5, hydrolysis and carbonate complexation reactions dominate the speciation in solution with a species distribution of 31% NpO_2^+, 11% NpO_2OH, and 58% $NpO_2CO_3^-$. Thus, to avoid the combined uncertainties of their formation constants and the non-steady-state behavior at pH 8.5, only the solubility data at pH 6 and pH 7 were used. At pH 6 and 7 and 2.8 mmol total carbonate, Np(V) hydrolysis and carbonate complexation reactions are minimized (*22*, *24*) and NpO_2^+ is the predominant solution species (100% and 94%, respectively). From the undersaturation data set, a mean thermodynamic solubility product $\log K^\circ_{sp} = 5.2 \pm 0.8$ was calculated for reaction 1:

$$Np_2O_5 \cdot xH_2O + 2H^+ \rightleftharpoons 2NpO_2^+ + (x+1)H_2O \qquad (1)$$

Note that at these low ionic strengths the water activity does not change the ΔG° (or K°_{sp}) calculated for the reaction and the solubility product is given by $K^\circ_{sp} = \{NpO_2^+\}^2/\{H^+\}^2$. Our value agrees well with that reported by Merli and Fuger, $\log K^\circ_{sp} = 5.5 \pm 1.9$, which was calculated from calorimetric data (*30*). However, both values imply a significantly lower logarithmic thermodynamic solubility product from the value 9.5 (*15*) thus far used in the EQ3/6com database, lowering the calculated neptunium solubility by several orders of magnitude.

Plutonium Solubility. The plutonium solubility was studied only from oversaturation (Table 4). In general, plutonium is about 3 orders of magnitude less soluble than neptunium, and pH does not affect the soluble concentration as much as seen in the neptunium solubility studies (Figure 3). Increasing temperature decreases the plutonium solubility below 10^{-8} mol L^{-1}. The plutonium concentrations at 60 and 90 °C are pH independent, while at 25 °C they show higher variability. Note that the solutions were filtered through 4.1-nm pore size filters and that the solubility data include the possible presence of small-sized plutonium colloids. Thus, the listed plutonium solubility data are conservative with respect to the real solid−liquid phase equilibria with soluble molecular species.

The plutonium precipitates were dark green, characteristic of Pu(IV) solid phases. Most of the observed X-ray diffraction

TABLE 4. Averaged Concentrations of $^{239/240}Pu$ (in mol L^{-1}) as a Function of pH and Temperature As Measured from Oversaturation (after 400 days Equilibration) in This Study in Comparison with Literature Data (*6*, *7*)[a]

	pH 6	pH 7	pH 8.5
25 °C			
oversaturation	$(4.7 \pm 1.1) \times 10^{-8}$	$(2.4 \pm 1.2) \times 10^{-8}$	$(9.4 \pm 1.6) \times 10^{-9}$
[lit.]	$(1.1 \pm 0.4) \times 10^{-6}$	$(2.3 \pm 1.4) \times 10^{-7}$	$(2.9 \pm 0.8) \times 10^{-7}$
60 °C			
oversaturation	$(9.0 \pm 2.0) \times 10^{-9}$	$(8.2 \pm 0.7) \times 10^{-9}$	$(6.2 \pm 1.8) \times 10^{-9}$
[lit.]	$(2.7 \pm 1.1) \times 10^{-8}$	$(3.8 \pm 0.9) \times 10^{-8}$	$(12 \pm 1) \times 10^{-8}$
90 °C			
oversaturation	$(4.3 \pm 2.1) \times 10^{-9}$	$(3.6 \pm 1.1) \times 10^{-9}$	$(4.2 \pm 1.1) \times 10^{-9}$
[lit.]	$(6.2 \pm 1.9) \times 10^{-9}$	$(8.8 \pm 0.8) \times 10^{-9}$	$(7.3 \pm 0.4) \times 10^{-9}$

[a] Uncertainties are given as 1 SD.

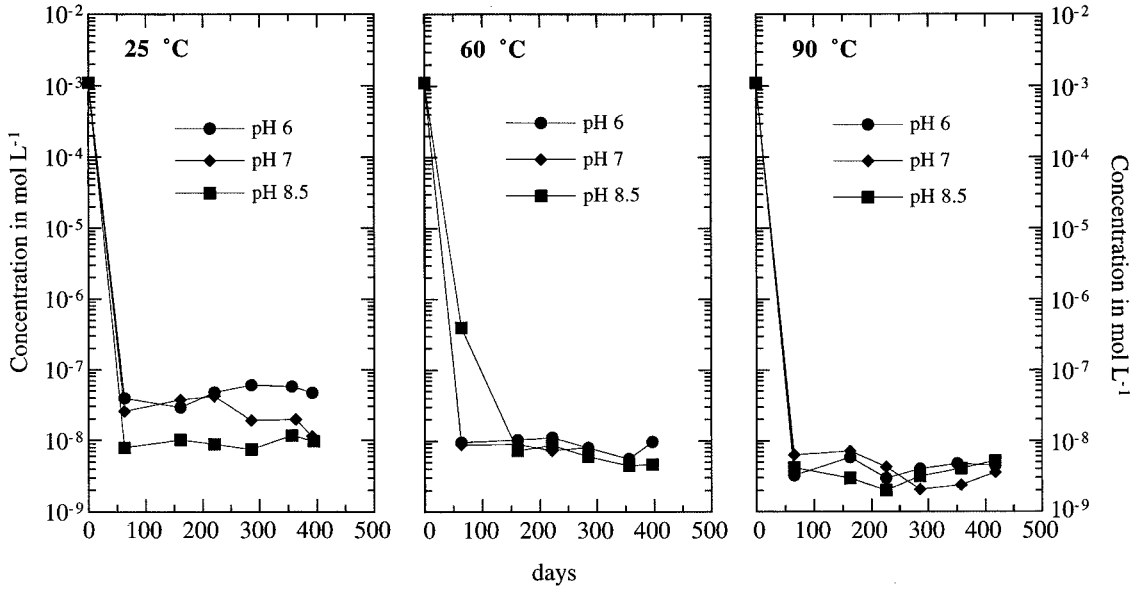

FIGURE 3. Plutonium solubility in J-13 water from oversaturation at (●) pH 6, (◆) 7, and (■) 8.5 and 25, 60, and 90 °C.

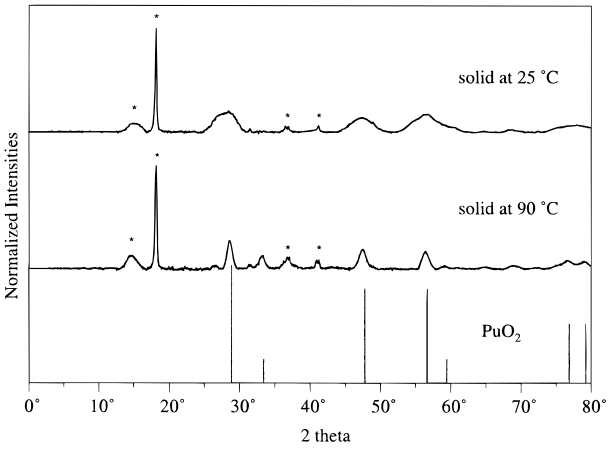

FIGURE 4. X-ray diffraction pattern of the plutonium solid found in J-13 water at 25 and 90 °C in comparison with literature data of PuO_2. Bragg reflections caused by the sample arrangement are marked with an asterisk. The broad peak at about 15° arises from Kapton foil.

peaks were diffuse and broad, indicating the existence of a poorly crystalline solid phase (Figure 4). However, temperature increases the crystallinity of precipitates, and the powder diffraction patterns obtained for the solid formed at 90 °C have sharper Bragg reflections than observed for the low-temperature solids. The pattern matched the data reported for PuO_2 (*31*). However, this result does not exclude the potential presence of aged Pu(IV) polymer and/or amorphous $Pu(OH)_4$. Indeed, a rising absorption tail below 500 nm is observed in the diffuse reflectance spectrum of a precipitate formed at 90 °C, along with absorption peaks at 469, 510, 577, 610 (broad), and 735 nm, consistent with a Pu(IV) colloid precursor to PuO_2(s) (*31*). It has been reported previously that the diffuse reflectance spectra of Pu(IV) colloid and high-fired PuO_2 are similar (*32*). To investigate the potential presence of a carbonate solid, we dissolved the aged Pu(IV) solid in 3 M HCl. While the solid's color intensified to bright green with contact of the acidic solution, the solid dissolved only partially. The addition of HCl did not result in CO_2 gas evolution as would be expected if the solid were a carbonate salt. Interestingly, besides the expected Pu(IV) absorption at 469 nm, we observed a Pu(VI) absorption peak at 830 nm. Because oxidation of Pu(IV) to Pu(VI) did not occur during the time frame of this dissolution experiment, the observed Pu(VI) must have originated from the solid. Impurities of Pu(VI) in the solid may have formed radiolytically. In addition, the formation of a higher Pu oxidation state in PuO_2 is consistent with results from previous studies on the instability of PuO_2 in the presence of water vapor and the transformation to a mixed-valence plutonium(IV)/(VI) oxide layer at the solid surface (*33*, *34*). However, due to the instability of Pu(VI) in aqueous systems of low ionic strength and low redox potential, we do not expect a significant influence of Pu(VI) impurities in the solid on the plutonium bulk solubility. Plutonium hydroxides and/or plutonium colloids, aging toward $PuO_2 \cdot xH_2O$, are therefore interpreted to be the solubility-controlling solids in these experiments. The formation of these solid phases was also

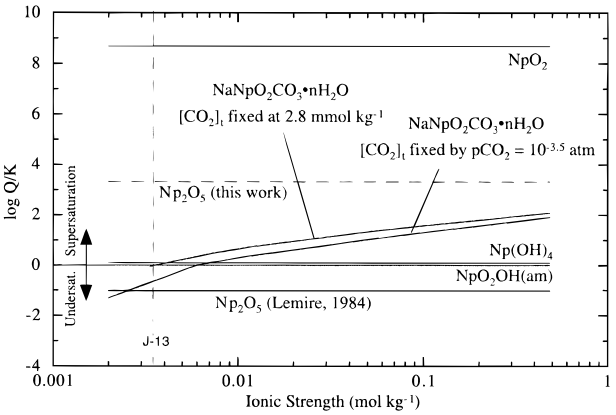

FIGURE 5. Calculated mineral saturation (log species product − log solubility product) at pH 7 as a function of ionic strength for solution speciation and solubility calculations. The redox potential was set to 430 mV, and charge balance was maintained with Na^+ or ClO_4^-.

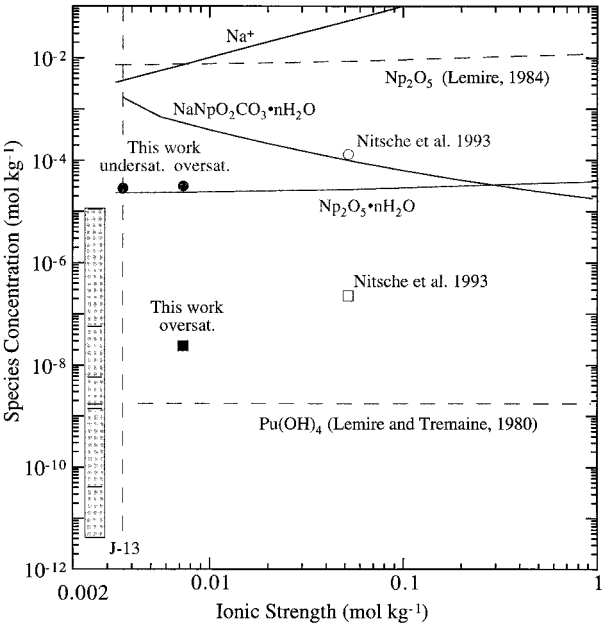

FIGURE 6. Comparison of experimental (○, ●) neptunium and (□, ■) plutonium solubilities in J-13 water at pH 7 and 430 mV with EQ3nr predictions. The carbonate concentration was fixed at 2.8 mmol kg-1. The box shows the range of Pu(IV) solubility calculated from $Pu(OH)_4$ solubility products taken from the literature (*41*−*46*). Note that PuO_2(c) would limit the plutonium solubility to ~10^{-17} mol kg-1, well distinct from the plutonium(IV) hydroxide solubility range.

reported previously in plutonium solubility measurements in Yucca Mountain water (*6*, *7*, *35*). Different crystallinities of the Pu(IV) colloidal material, possibly caused by different ionic strength or aging time, result in varying solubilities. A higher degree of amorphous material might be the reason for the slightly higher plutonium solubility reported previously (*6*, *7*) (Table 4).

Thermodynamic Modeling. Geochemical modeling using the EQ3nr aqueous speciation code was used to evaluate thermodynamic data for solution species and solid phases with respect to the experimental solubility measurements. The amount of dissolved solids in UZ waters from the YM area can differ by a factor of 2 (*36*), with J-13 water representing UZ waters at the lower end of the range. Consequently, the modeling was used to evaluate the influence of ionic strength on neptunium and plutonium solubility. Understanding the ionic strength effect is also important because of the experimental necessity to add NaOH and perchloric acid to J-13 water during initiation of the supersaturation solubility experiments. In one set of calculations, NpO_2OH(am) saturation was chosen as a reference, and its mineral saturation index was maintained at zero by adjusting the total neptunium concentration in solution (Figure 5). The calculations of neptunium solid phase saturation indicate a strong influence of the ionic strength only on the stability of $NaNpO_2CO_3 \cdot 3.5H_2O$ (Figure 5). The stability of the solid neptunium(V) carbonate increases with ionic strength and becomes supersaturated with respect to the calculated NpO_2OH(am) solubility controlling phase at ionic strengths between approximately 0.003 and 0.006 M, depending on the carbonate concentration in solution [saturation with atmospheric PCO_2 up to the 2.81 mmol measured in J-13 water (Table 1)]. Solid carbonates were reported previously to form in J-13 water at 25 and 60 °C, independent of the investigated pH, and at 90 °C at pH 7 and pH 8.5 (*6*, *7*). The predominant solid phases had been characterized by X-ray diffraction and identified as the sodium neptunium(V) carbonates, $Na_{0.6}NpO_2(CO_2)_{0.8} \cdot 2.5H_2O$, $NaNpO_2(CO_3) \cdot xH_2O$, and $Na_3NpO_2(CO_3)_2 \cdot xH_2O$. However, the stability of solid neptunium(V) carbonates is controlled by the neptunyl(V) carbonate, and sodium concentrations in solution as given by the apparent solubility product K_{sp}:

$$K_{sp}(Na_mNpO_2(CO_3)_n) = [Na^+]^m[NpO_2^+][CO_3^{2-}]^n \quad (2)$$

Since both sodium and carbonate concentrations in J-13 water are in the millimolar range (see Table 1), a very high Np(V) concentration (1 order of magnitude higher than those measured in this study) is needed to approach the solubility equilibrium of a neptunium(V) carbonate solid phase (Figure 6) (*17*). Indeed, the formation of $Na_3NpO_2(CO_3)_2 \cdot xH_2O$ can be definitely excluded at the low ionic strength of J-13 water (*17*). As suggested by our modeling studies (Figures 5 and 6), the reported anomalous appearance of the sodium neptunyl carbonates in J-13 water may be the result of an artificially high sodium concentration in those solubility experiments.

As described above, $Np_2O_5 \cdot xH_2O$ has been found in this study as the predominant solid phase formed in J-13. It was also reported to form together with an unidentified carbonate-containing solid phase at pH 5.9 and pH 7 at 90 °C in the earlier study (*6*, *7*, *37*). Based on the summarized relevant thermodynamic data in EQ3/6 (*15*, *16*), the more crystalline phase, $Np_2O_5 \cdot xH_2O$, is predicted to be undersaturated with respect to its amorphous hydration product NpO_2OH(am) (Figure 5). This contradicts the Gibbs' principle of minimizing free energy with crystallinity and suggests incorrect data in the thermodynamic database. Using the solubility product determined in this study, $\log K^\circ_{sp} = 5.2 \pm 0.8$, $Np_2O_5 \cdot xH_2O$ becomes supersaturated and less soluble than NpO_2OH(am) (dashed line in Figure 5).

Neptunium(IV) solids also are calculated to be less soluble than NpO_2OH(am), with NpO_2 as the most stable and insoluble solid phase (Figure 5). This solid has the potential to dominate the neptunium solubility under natural conditions (*38*−*40*). However, Np(IV) was not observed to form in these solubility experiments with Np(V) as the starting material, probably because of a kinetic barrier for the destruction of the *trans*-dioxo-neptunyl bonds, $(O{=}Np{=}O)^+$, and relatively high redox potentials in laboratory experiments. Thus, the data presented in this study provide upper solubility boundaries for radionuclide release scenario calculations. The calculated and experimentally determined solubility of neptunium and plutonium differ by several orders of magnitude mainly due to different oxidation states of the actinide in the solid state (Figure 6). Plutonium(IV) oxide/

hydroxide governs the plutonium solubility, while the higher soluble +V oxidation state determines the solubility of neptunium. Geochemical modeling using $Pu(OH)_4(s)$ as the solubility limiting solid phase ($\log K°_{sp} = -55.3$; *16*) resulted in a plutonium concentration of about 10^{-9} mol L^{-1} (Figure 6). The experimental data are about 1−2 orders of magnitude higher, but they lie within the broad solubility range calculated by using the solubility products for plutonium-(IV) hydroxide reported in the literature (gray bar in Figure 6) (*16*, *41*−*46*). In the case of the Pu(IV) system, it is hard to make accurate predictions due to the potential of the formation of the metastable Pu(IV) colloids and amorphous plutonium(IV) hydroxide solids. Both compounds span a wide range of structural features, crystallinities, stabilities, and solubilities.

The formation of hydrated Pu(IV) solids observed in this study also has implications for neptunium solubility calculations in natural environments. While the observed Np(V) solid, $Np_2O_5{\cdot}xH_2O$, is calculated to be metastable with respect to reduction to neptunium(IV) oxide, the formation of crystalline anhydrous NpO_2 in an aqueous system is rather unlikely. As in the plutonium case where hydrated forms of plutonium oxide/hydroxide were found, hydrated forms of neptunium(IV) oxide would likely form if the kinetic barrier to reduce Np(V) solids could be overcome. While dissolved plutonium is dominated by $Pu(OH)_4(aq)$ even at $E_h = 430$ mV, the geochemical behavior of neptunium differs from that of plutonium because solution speciation changes from NpO_2^+ at $E_h = 430$ mV to predominantly $Np(OH)_4(aq)$ by $E_h = 0$ mV. As a result, at 430 mV the solubility of neptunium-(IV) hydroxide is calculated to be in the same order as that of $Np_2O_5{\cdot}xH_2O$. The predicted solubility of $Np(OH)_4(s)$ at near-neutral pH can range between approximately 10^{-5} M at 430 mV to a minimum of about 10^{-8} M at 0 mV. Note that similar to $Pu(OH)_4(s)$, the range of K_{sp} for $Np(OH)_4(s)$ in the literature is huge, namely, ±4 orders of magnitude. This range translates directly into an uncertainty in the neptunium concentration if Np(IV) solids are formed. The measured neptunium concentration for such solids under reducing conditions is in the 10^{-6}−10^{-8} M range (*38*). These values are consistent with dissolution and solubility studies of neptunium-containing fuel rods (*47*−*50*), where the neptunium oxidation state in the starting material is +IV. Because infiltrating water into the repository is expected to be oxidizing (*36*, *40*, *51*), the use of Np(V) as a starting material is the conservative approach to provide defensible upper solubility boundaries. Studies are continuing on the possible reduction of the metastable Np(V) system in repository-like conditions further lowering the neptunium solubility source term. Experimental investigations of the solubility behavior of Np(V) and Np(IV) and the neptunium redox kinetics are critical to predicting neptunium transport in Yucca Mountain.

Acknowledgments

This work was supported by the Yucca Mountain Site Characterization Project Office of Los Alamos National Laboratory as part of the Civilian Radioactive Waste Management Program of the U.S. Department of Energy. The authors are grateful to Profs. Heinrich Holland (Harvard University) and Donald Langmuir, and Drs. Mary P. Neu (LANL) and David L. Clark (LANL) for helpful discussions.

Literature Cited

(1) Dozol, M.; Hagemann, R. *Pure Appl. Chem.* **1993**, *65*, 1081.
(2) Brooks, D. J.; Corrado, J. A. *Determination of Radionuclide Solubility in Groundwater for Assessment of High-Level Waste Isolation*; U.S. Nuclear Regulatory Commission: Washington, DC, 1984.
(3) Ogard, A. E.; Kerrisk, J. F. *Review of the groundwater chemistry along flow paths between a proposed repository site and the accessible environment*; Los Alamos National Laboratory: Los Alamos, NM, 1984.
(4) Hobart, D. E. In *Proceedings of the Robert A. Welch Conference on Chemical Research XXXIV. Fifty Years with Transuranium Elements*; Houston, TX, 1990; Chapter XIII, pp 379.
(5) DOE. General guidelines for the recommendation of sites for nuclear waste repositories. *Code of Federal Regulations*, Energy, Title 10, Part 960, 1988.
(6) Nitsche, H.; Gatti, R. C.; Standifer, E. M.; Lee, S. C.; Muller, A.; Prussin, T.; Deinhammer, R. S.; Maurer, H.; Becraft, K.; Leung, S.; Carpenter, S. A. *Measured solubilities and speciation of neptunium, plutonium, and americium in a typical groundwater (J-13) from the Yucca Mountain Region*; Lawrence Berkeley Laboratory: Livermore, CA, 1992.
(7) Nitsche, H.; Roberts, K.; Prussin, T.; Muller, A.; Becraft, K.; Keeney, D.; Carpenter, S. A.; Gatti, R. C. *Measured solubilities and speciations from oversaturated experiments of neptunium, plutonium, and americium in UE-25p#1 well water from the Yucca Mountain Site Characterization Program*; Lawrence Berkeley Laboratory: Livermore, CA, 1992.
(8) Andrews, R. W.; Dale, T. F.; McNeish, J. A. *Total System Performance Assessment−1993: An evaluation of the potential Yucca Mountain Repository*; INTERA, Inc.: 1994.
(9) Wilson, M. L.; Gauthier, J. G.; Barnard, R. W.; Barr, G. E.; Dockery, H. A.; Dunn, E.; Eaton, R. R.; Guerin, D. C.; Lu, N.; Martinez, M. J.; Nilson, R.; Rautman, C. A.; Robey, T. H.; Ross, B.; Ryder, E. E.; Schenker, A. R.; Shannon, S. A.; Skinner, L. H.; Halsey, W. G.; Gansemer, J. D.; Lewis, L. C.; Lamont, A. D.; Triay, I. R.; Meijer, A.; Morris, D. E. *Total-system performance assessment for Yucca Mountain−SNL second iteration (TSPA-1993)*; Sandia National Laboratories: 1994.
(10) DOE. *Site characterization plan, Yucca Mountain Site, Nevada Research and Development Area, Nevada*; Office of Civilian Radioactive Waste Management: 1988.
(11) Phillips, S. L.; Phillips, C. A.; Skeen, J. *Hydrolysis, formation and ionization constants at 25°C, and at high temperature-high ionic strength*; Lawrence Berkeley Laboratory: Livermore, CA, 1985.
(12) Wolery, T. J. *EQ3NR, A Computer Program for Geochemical Aqueous Speciation-Solubility Calculations: Theoretical Manual, User's Guide, and Related Documentation (Version 7.0)*; Lawrence Livermore National Laboratory: Livermore, CA, 1992.
(13) Wolery, T. J. *EQ3/6, A Software Package for Geochemical Modeling of Aqueous Systems: Package Overview and Installation Guide (Version 7.0)*; Lawrence Livermore National Laboratory: Livermore, CA, 1992.
(14) Helgeson, H. C. *Am. J. Sci.* **1969**, *267*, 729−804.
(15) Lemire, R. J. *An assessment of the thermodynamic behavior of neptunium in water and model groundwaters from 25 to 150°C*; Atomic Energy of Canada Limited: 1984.
(16) Lemire, R. J.; Tremaine, P. R. *J. Chem. Eng. Data* **1980**, *25*, 361−370.
(17) Neck, V.; Runde, W.; Kim, J. I. *J. Alloys Comp.* **1995**, *225*, 295−302.
(18) Runde, W.; Neu, M. P.; Clark, D. L. *Geochim. Cosmochim. Acta* **1996**, *60*, 2065−2073.
(19) Lemire, R. J.; Boyer, G. D.; Campbell, A. B. *Radiochim. Acta* **1993**, *61*, 57−63.
(20) Maya, L. *Inorg. Chem.* **1983**, *22*, 2093−2095.
(21) Maya, L. *Inorg. Chem.* **1984**, *23*, 3926−3930.
(22) Neck, V.; Kim, J. I.; Kanellakopulos, B. *Radiochim. Acta* **1992**, *56*, 25.
(23) Itagaki, H.; Nakayama, S.; Tanaka, S.; Yamawaki, M. *Radiochim. Acta* **1992**, *58/59*, 61−66.
(24) Lierse, C.; Treiber, W.; Kim, J. I. *Radiochim. Acta* **1985**, *38*, 27−28.
(25) Cohen, D. *Inorg. Chem.* **1963**, *2*, 866.
(26) Cohen, D.; Walter, A. J. *J. Chem. Soc.* **1964**, 2696−2699.
(27) Fahey, J. A. In *The Chemistry of the Actinide Elements*, 2nd ed.; Katz, J. J., Seaborg, G. T., Morss, L. R., Eds.; Chapman and Hall Publishers: New York, 1986; Vol. 1, pp 443−498.
(28) Belyaev, Y. I.; Solntsev, V. M.; Kapshukov, I. I.; Sudakov, L. V.; Chistyakov, V. M. *Radiokhimiya* **1974**, *16*, 747−752.
(29) JCPDS. *Powder Diffraction File, Alphabetical Index. Inorganic Phases. Diffraction Card No. 18-1436*; 1981.
(30) Merli, L.; Fuger, J. *Radiochim. Acta* **1994**, *66/67*, 109−113.
(31) Mooney, R. C. L.; Zachariasen, W. H. *The Transuranium Elements, Part II*; McGraw-Hill: New York, 1949; pp 1442−1447.
(32) Hobart, D. E.; Morris, D. E.; Palmer, P. D.; Newton, T. In *Nuclear Waste Isolation in the Unsaturated Zone, Focus '89*; American Nuclear Society: La Grange Park, IL, 1990; pp 118−124.
(33) Stakebake, J. L.; Larson, D. T.; Haschke, J. M. *J. Alloys Comp.* **1993**, *202*, 251−263.

(34) Haschke, J. M.; Ricketts, T. E. *J. Alloys Comp.* **1997**, *252*.
(35) Nitsche, H.; Muller, A.; Standifer, E. M.; Deinhammer, R. S.; Becraft, K.; Prussin, T.; Gatti, R. C. *Radiochim. Acta* **1992**, *58*/*59*, 27−32.
(36) Yang, I. C.; Rattray, G. W.; Yu, P. *Interpretations of Chemical and Isotopic Data from Bore Holes in the Unsaturated-Zone at Yucca Mountain, Nevada*; U.S. Geol. Survey Water-Resources Inventory, USGS: Denver, 1996.
(37) Nitsche, H. *Inorg. Chim. Acta* **1987**, *127*, 121.
(38) Rai, D.; Ryan, J. L. *Inorg. Chem.* **1985**, *24*, 247−251.
(39) Rai, D.; Swanson, J. L.; Ryan, J. L. *Radiochim. Acta* **1987**, *42*, 35−41.
(40) Langmuir, D. *Aqueous Environmental Geochemistry*; Prentice Hall: Upper Saddle River, NJ, 1997.
(41) Pazhukin, E. M.; Kudryavtsev, E. G. *Sov. Radiochem.* **1990**, *32*, 318.
(42) Kim, J. I.; Kanellakopulos, B. *Radiochim. Acta* **1989**, *48*, 145.
(43) Lierse, C.; Kim, J. I. *Chemisches Verhalten von Plutonium in Natürlichen Aquatischen Systemen: Hydrolyze, Carbonatkomplexierung und Redoxreaktionen*; TU: Munich, 1986.
(44) Rai, D. *Soil. Sci. Soc. Am. J.* **1980**, *44*, 490.
(45) Rai, D. *Radiochim. Acta* **1984**, *35*, 97.
(46) Kasha, M. In *The Transuranium Elements*; Seaborg, G. T., Ed.; McGraw-Hill: New York, 1949; p 328.
(47) Wilson, T. J.; Bruton, C. J. In *Nuclear Waste Management. III. Ceramic Transactions*; American Ceramic Society: Westerville, OH, 1990; pp 423−441.
(48) Wilson, C. N. *Results from NNWSI Series 3 Spent Fuel Dissolution Tests*; Pacific Northwest Laboratory, 1990.
(49) Bruton, C. J.; Shaw, H. J. In *Mater. Res. Soc. Symp.* **1988**, pp 485−494.
(50) Finn, P. A.; Hoh, J. C.; Wolf, S. F.; Slater, S. A.; Bates, J. K. *Radiochim. Acta* **1996**, *75*, 65−71.
(51) Yang, I. C. *3rd International Conference on High Level Radioactive Waste Management*; American Nuclear Society: La Grange Park, IL, 1992; pp 732−737.

Received for review June 9, 1998. Revised manuscript received September 23, 1998. Accepted September 25, 1998.

ES980591H